Citation: CPT Pharmacometrics Syst. Pharmacol. (2018) 7, 374–383; doi:10.1002/psp4.12295

ARTICLE

First-Pass CYP3A-Mediated Metabolism of Midazolam in the Gut Wall and Liver in Preterm Neonates

Janneke M. Brussee[1], Huixin Yu[1], Elke H. J. Krekels[1], Berend de Roos[1], Margreke J. E. Brill[2], Johannes N. van den Anker[3,4,5], Amin Rostami-Hodjegan[6,7], Saskia N. de Wildt[3,8] and Catherijne A. J. Knibbe[1,9]*

To predict first-pass and systemic cytochrome P450 (CYP) 3A-mediated metabolism of midazolam in preterm neonates, a physiological population pharmacokinetic model was developed describing intestinal and hepatic midazolam clearance in preterm infants. On the basis of midazolam and 1-OH-midazolam concentrations from 37 preterm neonates (gestational age 26–34 weeks) receiving midazolam orally and/or via a 30-minute intravenous infusion, intrinsic clearance in the gut wall and liver were found to be very low, with lower values in the gut wall (0.0196 and 6.7 L/h, respectively). This results in a highly variable and high total oral bioavailability of 92.1% (range, 67–95%) in preterm neonates, whereas this is around 30% in adults. This approach in which intestinal and hepatic clearance were separately estimated shows that the high bioavailability in preterm neonates is explained by, likely age-related, low CYP3A activity in the liver and even lower CYP3A activity in the gut wall.

CPT Pharmacometrics Syst. Pharmacol. (2018) **7**, 374–383; doi:10.1002/psp4.12295; published online 10 May 2018.

Study Highlights

WHAT IS THE CURRENT KNOWLEDGE ON THE TOPIC?

☑ That the CYP enzymes are present in the gut wall and liver, but a different contribution of the gut and the liver to the first-pass effect may be anticipated in children as compared with adults, due to different rates of maturation of intestinal and hepatic enzymes in infants and children.

WHAT QUESTION DID THIS STUDY ADDRESS?

☑ That first-pass metabolism in the gut wall and liver can be predicted for the CYP3A substrate midazolam using a state-of-the-art physiological population PK modeling approach.

WHAT DOES THIS STUDY ADD TO OUR KNOWLEDGE?

☑ A very low first-pass effect by intestinal and hepatic CYP3A-mediated metabolism was found for midazolam in preterm neonates, yielding much higher bioavailability of midazolam in preterm neonates compared with adults. Furthermore, intestinal CYP3A activity, represented by intrinsic clearance in the gut wall, was much lower than hepatic CYP3A activity, represented by the intrinsic clearance in the liver.

HOW MIGHT THIS CHANGE DRUG DISCOVERY, DEVELOPMENT, AND/OR THERAPEUTICS?

☑ Characterization of gut wall and hepatic CYP3A activity enables quantitative predictions of first-pass and systemic metabolism of midazolam and potentially other CYP3A substrates in preterm neonates.

The neonatal body is undergoing many dynamic changes in the first months of life,[1] with preterm neonates showing delayed maturation of many organs as compared with term neonates. This results among others in an altered and highly variable capacity to deal with xenobiotics, including drugs.[2,3] Metabolic capacity is an important determinant for the bioavailability and systemic clearance of drugs that are subject to metabolic clearance. Bioavailability impacted by intestinal and hepatic metabolism and systemic clearance impacted by hepatic metabolism are the two main drivers of drug exposure. Interindividual differences in these two parameters are, therefore, two of the main drivers of differences in drug dose requirements between patients.

Physiological parameters that affect drug metabolism include protein binding, blood flow, and intrinsic clearance, the latter of which represents metabolic capacity.[3,4] Developmental changes in albumin concentrations[5] and drug protein binding[6] have been reported in neonates, as well as changes in cardiac output,[5] which influence the intestinal and hepatic blood flow.[7] However, there is limited knowledge on the development of intrinsic clearance of many drugs, especially with respect to the intestinal and hepatic enzyme activity in preterm infants.

[1]Division of Systems Biomedicine and Pharmacology, Leiden Academic Centre for Drug Research (LACDR), Leiden University, Leiden, The Netherlands; [2]Department of Pharmaceutical Biosciences, Uppsala University, Uppsala, Sweden; [3]Intensive Care and Department of Pediatric Surgery, Erasmus MC - Sophia Children's Hospital, Rotterdam, The Netherlands; [4]Division of Paediatric Pharmacology and Pharmacometrics, University of Basel Children's Hospital, Basel, Switzerland; [5]Division of Clinical Pharmacology, Children's National Health System, Washington, DC; [6]Centre for Applied Pharmacokinetic Research, University of Manchester, Manchester, UK; [7]Simcyp Limited (A Certara Company), Sheffield, UK; [8]Department of Pharmacology and Toxicology, Radboud University Medical Centre, Nijmegen, The Netherlands; [9]Department of Clinical Pharmacy, St. Antonius Hospital, Nieuwegein, The Netherlands. *Correspondence: Catherijne Knibbe (c.knibbe@antoniusziekenhuis.nl)
Received 9 February 2018; accepted 9 March 2018; published online on 10 May 2018. doi:10.1002/psp4.12295

Cytochrome P450 (CYP) is an enzyme family involved in drug metabolism and its ontogeny in children has been studied both *in vitro* and *in vivo*.[8] The CYP3A subfamily (i.e., CYP3A4, CYP3A5, and CYP3A7) is involved in metabolism of many clinical important drugs with midazolam commonly used as a probe drug to reflect combined CYP3A activity.[9,10] Midazolam is a benzodiazepine, often used for sedation in the neonatal intensive care unit,[11] and its CYP3A-mediated clearance have been reported to be lower in neonates, infants, and children, compared with adults.[12] As CYP3A resides in both the gut wall and the liver,[13] it is of interest to distinguish between intestinal and hepatic CYP3A activity with respect to their roles in first-pass metabolism, particularly because intestinal and hepatic enzymes may mature at different rates. Besides CYP3A activity in the gut wall and liver, important factors that may affect the absorption and metabolism of drugs in the gut wall are among others the intestinal surface area and the permeability of the endothelium.[14] Preterm infants have a smaller surface area and are known to have an underdeveloped intestinal barrier,[15] resulting in a higher intestinal permeability in neonates with gestational ages of $<$34 weeks.[16]

To describe and predict pharmacokinetic (PK) profiles and drug exposure in patients, different types of models have been used based on availability of data and their purpose. These models range from relatively simple, empirical models, to more complex (semi-)physiologically based PK models.[17] Empirical models often lack predictive value outside the studied population, whereas large physiologically based pharmacokinetic models are not always identifiable and may depend on system parameters that are difficult to determine experimentally in children. Therefore, a hybrid of these models is useful not only to determine PK of a single drug but also to obtain insight into drug independent systems information when the models are used for several drugs simultaneously.[18] In this analysis, we used a physiological population PK modeling approach, in which we account for the attributes of the gastrointestinal tract and use available systems data together with PK information from the preterm population to describe intestinal and hepatic midazolam clearance and ultimately predict first-pass and systemic metabolism by CYP3A of midazolam in preterm neonates.

METHODS

Data

Thirty-seven preterm neonates (gestational ages ranging from 26–34 weeks, birth weights 745–2,135 grams) of a previously published dataset from the neonatal intensive care unit of the Sophia's Children Hospital in Rotterdam were included.[19,20] At the time of the clinical investigation, their postnatal ages ranged from 3–11 days and their body weights between 770 and 2,030 grams. These infants were randomly assigned to receive 0.1 mg/kg midazolam orally via a nasogastric tube ($n = 13$) or intravenously via a 30-minute infusion ($n = 25$). If, after 72 hours, the participating infants still met the inclusion criteria, they received another dose of midazolam but this time via the other route. Midazolam and its primary metabolite 1-OH-midazolam were measured in plasma 0.5, 1, 2, 4, 6, 12, and 24 hours postdose[19,20] and measurements below the lower limit of quantification were discarded ($<$1% and $<$2% of 329 and 153 midazolam and 1-OH-midazolam measurements, respectively).

Model development

Structural physiological pharmacokinetic model. Physiological population PK modeling was performed using first-order conditional estimation with interaction in NONMEM version 7.3 (ICON, Globomax, Ellicott, MD) with Pirana 2.9.0 and R (version 3.3.1) and R-studio (version 0.98.1078) for processing of the runs and visualization of data.

A physiological population PK model, earlier described by Yang *et al.*,[21] Frechen *et al.*,[22] and Brill *et al.*,[23] was applied to describe the data (**Figure 1**). For this, using the blood: plasma ratio and the measured molar concentrations in plasma, the drug and metabolite molar concentrations in blood were calculated to be able to be used in the well-stirred model. The model describes physiological compartments representing the gut wall, the portal vein, and the liver, and an empirical central compartment for midazolam and 1-OH-midazolam, representing the blood circulation and equilibrating tissue.[21,22] For midazolam and 1-OH-midazolam, also the addition of empirical peripheral compartments was evaluated. The fraction of midazolam metabolized into 1-OH-midazolam was assumed to be 1.

Tissue volumes for the physiological compartments in the preterm neonatal population were allometrically scaled from tissue volumes of a term neonate[7] with a fixed exponent of 1 (**Table 1** [5–7,24–31,48]). Volume of the portal vein was assumed to be 77.8% of the hepatic volume.[24] The hepatic blood flow was assumed to allometrically scale from a term neonate[7] with a fixed exponent of 0.75. Blood flows in the other tissues were assumed to be proportional to the hepatic blood flow (**Table 1**[5,7,25,32]).

The well-stirred model was used to quantify the hepatic extraction of midazolam (E_H) and 1-OH-midazolam ($E_{H,M}$):

$$E_H = \frac{CL_{int,H} \times f_{u,B}}{Q_h + \left(CL_{int,H} \times f_{u,B}\right)} \quad (1)$$

where $CL_{int,H}$ is the estimated intrinsic clearance in the liver based on unbound blood concentrations, $f_{u,B}$ is the fraction unbound drug concentration in blood, and Q_h is the hepatic blood flow.

For gut wall metabolism into 1-OH-midazolam (E_G), the Q_{gut} model was applied[25]:

$$E_G = \frac{CL_{int,G} \times f_{u,G}}{Q_{gut} + \left(CL_{int,G} \times f_{u,G}\right)} \quad (2)$$

where $CL_{int,G}$ is the estimated intrinsic clearance in the gut wall based on unbound concentrations, $f_{u,G}$ is the fraction unbound drug concentration in the gut wall, and Q_{gut} is the local blood flow, which is defined by[25]:

$$Q_{gut} = \frac{Q_{villi} \times CL_{perm}}{Q_{villi} + CL_{perm}} \quad (3)$$

where Q_{villi} is the villous blood flow and CL_{perm} is the permeability of the drug through the enterocytes in the gut

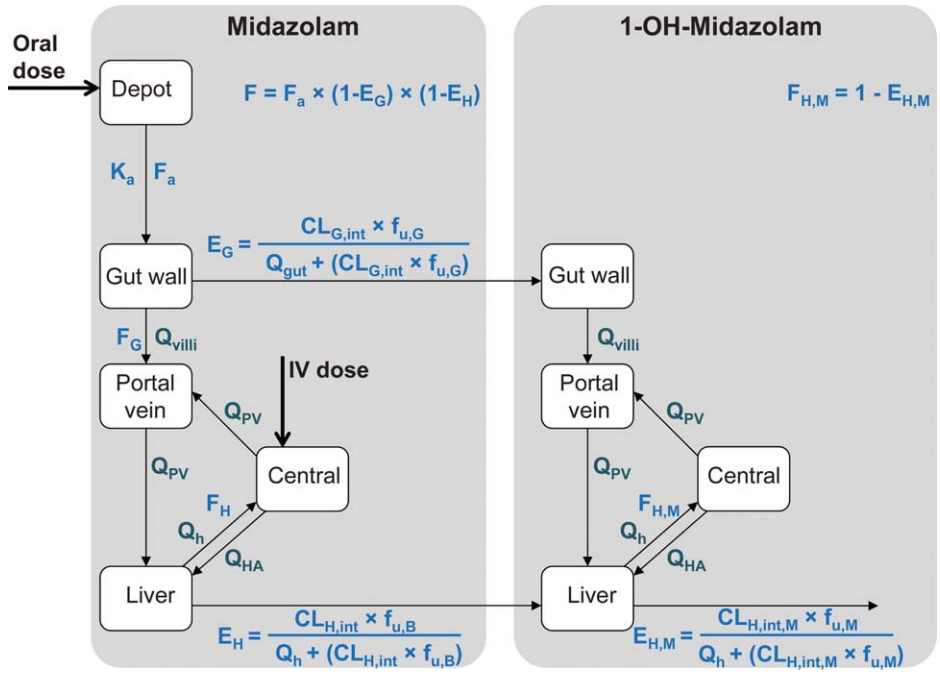

Figure 1 Schematic representation of the model for midazolam and the 1-OH-midazolam metabolite. CL_{int}, the intrinsic clearance in the blood; E, extraction ratio; F, bioavailability in the gut wall (gut, G) and the liver (hepatic, H); K_a indicates the absorption rate constant and the fraction unbound in blood and gut wall are described with $f_{u,B}$ and $f_{u,G}$, respectively. Blood flows are represented by Q; in the micro villi (Q_{villi}), portal vein (Q_{PV}), hepatic artery (Q_{HA}), and the hepatic blood flow (Qh). Parameters relating to the metabolite are indicated with subscript M. Intrinsic gut wall ($CL_{G,int}$) and intrinsic hepatic clearance ($CL_{H,int}$ and $CL_{H,int,M}$), as well as volume of distribution (for midazolam and 1-OH-midazolam), values were estimated in the model. Total plasma clearance of midazolam was derived using Eq. 8, and the bioavailability in the gut wall (F_g), liver (F_h), and the total oral bioavailability (F_{total}) were derived based on Eqs. 1, 2, and 5.

wall, which depends on the effective intestinal permeability per unit surface area[25] and the intestinal surface area. The intestinal surface area (A) was calculated based on the net cylindrical surface area of the small intestine using Eq. 4.

$$A = 2\pi \times r \times h \tag{4}$$

in which r is the intestinal radius of 1 cm,[26] and h the intestinal length of $2.736 \times (WT[g])^{0.512}$ cm.[27] The fraction unbound in the gut ($f_{u,G}$) for both midazolam and 1-OH-midazolam was assumed 1.[25] The absorption rate constant could not be estimated and was assumed to be 10 h^{-1}, which entails an expected maximum concentration around 12.5 minutes (time of maximum plasma concentration (T_{max})). A sensitivity analysis was performed with values for k_a ranging from 4.16–25 h^{-1}, resulting in a T_{max} between 5 and 30 minutes postdose. The oral bioavailability was calculated with Eq. 5:

$$F_{total} = F_a \times F_g \times F_h \tag{5}$$

where F_a is the fraction absorbed, which is assumed 1 for midazolam,[10] F_g is the gut wall bioavailability, equal to 1 minus E_g, and F_h is the hepatic bioavailability, and $F_h = 1 - E_h$.

The fraction unbound in blood for both midazolam and 1-OH-midazolam in blood was calculated based on the formula of McNamara and Alcorn[6]:

$$f_{u,B,pediatric} = \frac{1}{1 + \frac{(1 - f_{u,B,adult}) \times [P]_{pediatric}}{[P]_{adult} \times f_{u,B,adult}}} \tag{6}$$

where $f_{u,pediatric}$ and $f_{u,adult}$ are the fraction unbound of the drug in blood for preterm neonates and adults, respectively, and $[P]_{pediatric}$ and $[P]_{adult}$ are the plasma albumin concentrations in preterm neonates and adults, respectively. These albumin concentrations are calculated based on an age-based formula from Johnson *et al.*[5] (**Table 1**) and the fractions unbound of midazolam and 1-OH-midazolam in adults were reported in literature.[28,29] The fraction unbound in blood and hematocrit were used to calculate the blood: plasma ratios for midazolam and 1-OH-midazolam using the formula of Maharaj *et al.*[30]:

$$B : P \text{ ratio} = 1 + [Hem \times (fu, B \times Kp - 1)] \tag{7}$$

where B:P ratio is the blood:plasma ratio, Hem is the hematocrit in preterm neonates (45%),[31] $f_{u,B}$ is the fraction unbound in the blood, and K_p is the unbound partition coefficient of red blood cells (assumed to be constant between adults and children).[30]

Total plasma clearance by the liver was calculated based on[33]:

$$CL_{plasma} = \frac{Q_h \times f_u \times CL_{h,int}}{Qh + (f_u \times CL_{h,int} / (B : P \text{ ratio}))} \tag{8}$$

Table 1 Parameter values for physiological and drug specific parameters in the model

Parameter definition (unit)	Parameter	Formula for calculation	Value	References
Tissue volumes (L)				
Liver	V_h	$V_{h,3.55kg\ neonate} \times (WT/3.55)$		(7)
		$V_{h,3.55kg\ neonate} = 0.120$		
Portal vein	V_{pv}	$V_{pv} = 0.778 \times V_h$		(24)
Gut	V_{gw}	$V_{gw,3.55kg\ neonate} \times (WT/3.55)$		(7)
		$V_{gw,3.55kg\ neonate} = 0.050$		
Tissue blood flows (L/h)				
Hepatic blood flow	Q_h	$Q_{h,3.55kg\ neonate} \times (WT/3.55)^{0.75}$		(7)
		$Q_{h,3.55kg\ neonate} = 13.2$		
Portal vein	Q_{pv}	$0.75 \times Q_h$		(5, 32)
Hepatic artery	Q_{ha}	$0.25 \times Q_h$		(5, 32)
Small intestine	Q_{in}	$0.4 \times Q_h$		(25)
Mucosa	Q_{muc}	$0.8 \times Q_{in}$		(25)
Microvilli	Q_{villi}	$0.6 \times Q_{muc}$		(25)
Plasma proteins				
Plasma albumin concentration (g/L)	$[P]_{pediatric}$	$1.1287 \times \ln(Age[yr]) + 33.746$	27.1	(5)
	$[P]_{adult}$		37.0	
Hematocrit (%)	Hem	–	0.45	(31)
Intestinal surface area and permeability				
Intestinal surface area (dm^2)	A	$2\pi \times r \times h$	5.97	r: (26)
		With radius r = 1 cm and length $h = 2.736 \times (WT[g])^{0.512}$ cm		h: (27)
Permeability through the enterocyte (L/h)	CL_{perm}	$CL_{perm} = P_{eff,man}$ [dm/h] × A [dm^2]	0.95	(25)
Midazolam				
Fraction absorbed	F_a	–	1	(10)
Absorption rate constant	K_a (h^{-1})	–	10	–
Blood:plasma ratio	B:P ratio	$1 + [Hem \times (f_{u,B} \times K_p - 1)]$ $K_p = 1$	0.568	(30)
Fraction unbound in gut	$F_{u,G}$	–	1	(25)
Fraction unbound in blood	$F_{u,B}$	$\frac{1}{1+\frac{(1-f_{u,adult})\times[P]_{pediatric}}{[P]_{adult}\times f_{u,adult}}}$	0.04094	(6)
	$F_{u,adult}$		0.0303	(28)
Effective intestinal permeability per unit surface area (cm/s)	$P_{eff,man}$	–	4.4×10^{-4}	(25)
1-OH-midazolam				
Fraction midazolam metabolized into 1-OH-midazolam	f_M	–	1	–
Blood:plasma ratio	B:P ratio	$1 + [Hem \times (f_{u,M} \times K_p - 1)]$ $K_p = 1$	0.613	(30)
Fraction unbound in blood	$F_{u,M}$	$\frac{1}{1+\frac{(1-f_{u,M,adult})\times[P]_{pediatric}}{[P]_{adult}\times f_{u,M,adult}}}$	0.1394	(6)
	$f_{u,M,adult}$		0.106	(29)

in which Q_h is the hepatic blood flow, f_u the fraction unbound in plasma, and $CL_{h,int}$ the intrinsic hepatic clearance.

To evaluate the structural identifiability or our nonlinear model, we used the Differential Algebra for Identifiability of Systems software.[34]

Statistical model

Interindividual variability was included in the model as a log-normal distribution:

$$\theta_i = \theta_{TV} \times e^{\eta_i} \quad (9)$$

where θ_i is individual parameter estimate for individual *i*, θ_{TV} is the typical value of the parameter in the studied population, and η_i is a random variable from a normal distribution with a mean of zero and estimated variance of ω^2.

Residual unexplained variability was modeled using a combined error model. The *j*th observed concentration (Y) of the *i*th individual was modeled according to:

$$Yij = Cpred,ij \times (1+\varepsilon 1ij) + \varepsilon 2ij \quad (10)$$

where $C_{pred,ij}$ is the *j*th predicted midazolam concentration of the *i*th individual, $\varepsilon 1_{ij}$ and $\varepsilon 2_{ij}$ are random variables from normal distributions with a mean of zero and estimated variance of σ^2, representing the proportional and additive component of the error model, respectively.

Covariate analysis

A covariate analysis on the clearance and volume parameters was performed in which the following covariates were tested for statistical significance: body weight at birth, gestational age, gender, and mechanical respiratory support, and furthermore body weight, postmenstrual age, and postnatal age per occasion (e.g., at the day of dose administration). There was no missing covariate information for any subject.

For categorical covariates, separate typical values (θ_{TV}) for the two populations were estimated. Continuous covariates were tested using a linear (Eq. 11) or power (Eq. 12) function.

$$\theta_i = \theta_{TV} \times (1+\theta_{cov} \times (COV - COV_{med}) \quad (11)$$

$$\theta_i = \theta_{TV} \times \left(\frac{COV}{COVmed}\right)^{\theta_{cov}} \quad (12)$$

where θ_i is the individual parameter estimate for the individual *i*, θ_{TV} is the typical value of the parameter in the studied population with a median value (COV_{med}) of the covariate (COV), and θ_{COV} the estimated slope or exponent for a linear or power function, respectively.

Model evaluation

Discrimination between different structural models was made by comparison of the objective function value (OFV; i.e., $-2 \times$ log-likelihood). A decrease of 3.84 points in the OFV between nested models was considered statistically significant ($P < 0.05$). Furthermore, goodness-of-fit plots (individual-predicted and population-predicted vs. observed concentrations and conditional weighted residuals vs. time and population predicted concentrations) of midazolam and 1-OH-midazolam were assessed. In addition, the confidence interval of the parameter estimates and visual improvement of the individual plots were used to evaluate the models.

For inclusion of covariates, a decrease in OFV of 6.64 points ($P < 0.01$) was considered statistically significant, whereas for the backward deletion a more stringent *P* value ($P < 0.005$; ΔOFV >7.88) was used. Furthermore, to retain a covariate in the model, the interindividual variability in the PK parameter should decrease and in a plot of the covariate vs. the interindividual variability in the PK parameter, the data points should be randomly scattered around zero.

The model was further internally evaluated using two different methods, a bootstrap analysis ($n = 200$) and a normalized prediction distribution error analysis (see **Supplementary Figures S1 and S2**).

Sensitivity analysis

To evaluate the assumptions made in the model, a sensitivity analysis was performed using simulations in Berkeley Madonna software (Berkeley Madonna, version 8.3.18).[35] Parameter values for tissue volumes and blood flows as well as intestinal length and the fraction unbound in blood were increased and decreased by 50% and the impact on predicted midazolam concentrations was evaluated. Furthermore, the impact of the assumptions on the estimated PK parameters was assessed by re-estimating the model with the increased/decreased values for tissue volumes and blood flows as well as intestinal length and the fraction unbound in blood.

Dose simulations

To illustrate the impact of first-pass metabolism on midazolam and 1-OH-midazolam exposure in preterm neonates, model-based simulations of concentration-time profiles were performed with our model. A dose of 0.1 mg/kg midazolam was simulated as oral administration or as a 30-minute intravenous infusion in 37 preterm neonates with the same patient characteristics as the individuals in our dataset.

RESULTS

Using the physiological population PK model, as depicted in **Figure 1**, which was structurally identifiable according to the Differential Algebra for Identifiability of Systems analysis,[34] the PK data in preterm neonates were well described. Based on the available data, intrinsic CYP3A clearance in the gut wall and liver were estimated to be 0.0196 (relative standard error (RSE) 178%) and 6.7 (RSE 10%) L/h, respectively (**Table 2**). Distribution volumes for midazolam and its metabolite in blood were estimated to be 3 (RSE 11%) and 2.7 (RSE 43%) L, respectively, and the addition of peripheral compartments for either midazolam or 1-OH-midazolam did not improve the model. No additional covariates could be identified for intrinsic clearance and volume of distribution. The model was graphically and numerically evaluated (**Table 2, and Supplementary Figures S1 and S2**) and generally the model parameters described the PK data of both the midazolam and 1-OH-midazolam well. The additive errors were fixed to very small numbers (**Table 2**). Goodness-of-fit plots (**Supplementary Figure S1**) showed that the model adequately describes the data, albeit with a

Table 2 Parameter estimates and bootstrap results of the physiological population PK model

Parameter definition	Parameter	Value (RSE%) [shrinkage %]	Bootstrap median[a]	Bootstrap 90% CI
Midazolam				
Intrinsic hepatic clearance	$CL_{H,int}$ (L/h)	6.7 (10)	6.6	5.0–8.7
Intrinsic gut wall clearance	$CL_{G,int}$ (mL/h)	19.6 (178)	14.0	0.2[b]–319
Volume of distribution	V (L)	3.0 (11)	3.0	2.4–3.7
1-OH-midazolam				
Intrinsic hepatic clearance	$CL_{H,int,M}$ (L/h)	8.9 (22)	7.7	3.5–11.2
Volume of distribution	V_M (L)	2.7 (43)	2.9	1.5–7.2
Interindividual variability (ω^2)				
Intrinsic hepatic clearance	ω^2 $CL_{H,int}$	0.887 (26) [3]	0.851	0.551–1.16
Intrinsic gut wall clearance	ω^2 $CL_{G,int}$	–	–	–
Volume of distribution	ω^2 V	0.603 (26) [2]	0.603	0.311–0.857
Intrinsic hepatic clearance 1-OH-midazolam	ω^2 $CL_{H,int,M}$	0.832 (42) [15]	0.709	0.201–1.65
Volume of distribution 1-OH-midazolam	ω^2 V_M	0.887 (48) [8]	1.2	0.442–4.04
Residual variability (σ^2)				
Proportional error (midazolam)		0.201 (26) [10]	0.192	0.134–0.264
Additional error (midazolam)		0.0001 FIX	0.0001	–
Proportional error (1-OH-midazolam)		0.164 (91) [33]	0.155	0.000[b]–0.242
Additional error (1-OH-midazolam)		0.0001 FIX	0.0001	–

CI, confidence interval; PK, pharmacokinetic; RSE, relative standard error.
[a]Bootstrap results based on stratified bootstrap sampling for patients receiving an intravenous, an oral, or twice a dose administration. The median and 90% confidence interval are calculated based on 37.8% successful runs and runs with estimates near a boundary.
[b]The 5% percentile reached the lower boundary of 0.2 mL/h and $0.1*10^{-4}$, for $CL_{G,int}$ and the proportional error for 1-OH-midazolam, respectively. Interindividual and residual variability values are shown as variance estimates.

small overprediction for the low concentrations of midazolam. In addition, the prediction of the data was unbiased, as shown in the normalized prediction distribution error analysis (**Supplementary Figure S2**), with slightly overpredicted variability in the metabolite concentrations.

Intrinsic hepatic clearance was much higher and also more variable than the intrinsic gut wall clearance (**Figure 2a**). **Figures 2 and 3** show the estimated and derived model parameters related to the intestinal and hepatic metabolism in preterm neonates vs. bodyweight. The median total plasma clearance by the liver was 0.181 L/h (range 0.03–0.79 L/h; **Figure 2b**). As both the intrinsic gut wall and hepatic clearance were found to be very low (**Figure 2a**), the extraction ratios were very low for both organs, with a median of 0.04 in the gut wall (range 0.026–0.046) and a similar median of 0.04 (range 0.01–0.31) in the liver (**Figure 2c**). Based on the extraction ratio in the gut wall and liver, the fraction escaping gut wall metabolism (F_g) and the fraction escaping hepatic metabolism (F_h) can be calculated and the median values are both 0.96. **Figure 3** also shows the total bioavailability for all preterm neonates in our study, as calculated based on the fraction absorbed (F_a), F_g, and F_h according to Eq. 5. A very low first-pass metabolism was observed with 92% of midazolam entering the systemic circulation in a typical preterm neonate of 1.1 kg, but the overall range of percentage entering systemic circulation varies largely between 67% and 95%. Model-based simulations of plasma concentration-profiles show limited differences in median plasma concentrations of midazolam after oral and intravenous administration due to the high bioavailability of 92% (**Figure 4a**), whereas the concentrations of 1-OH-midazolam after oral administration are higher for the first 4 hours post-dose compared to the 30-minute infusion, due to presystemic metabolism (**Figure 4b**).

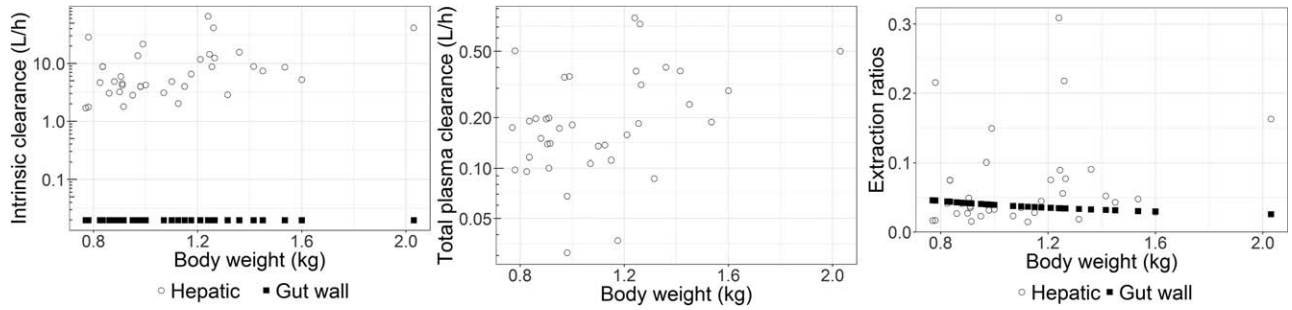

Figure 2 Intrinsic clearance (**a**), total plasma clearance (Eq. 8) (**b**) and extraction ratio (**c**) are plotted vs. body weight, in which values are given for the gut wall (■) and the liver (○).

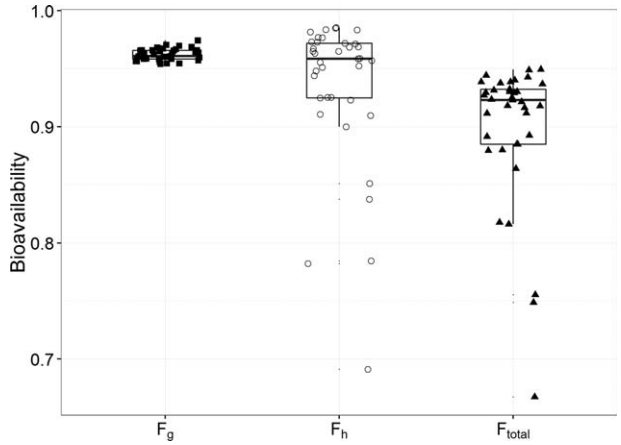

Figure 3 Bioavailability in the gut (F_g) and liver (F_h), and total bioavailability (F_{total}) in preterm neonates.

A sensitivity analysis showed that blood concentration predictions would change <1% for both peak and trough concentrations in case the values for tissue volumes and tissue blood flows were altered with ± 50%. In addition, no significant change in parameter estimates was found when the parameters were re-estimated based on the same changes in tissue volumes, nor did different k_a values impact estimated and derived clearance and bioavailability parameters. However, an increase of 50% in intestinal and hepatic blood flow resulted in an increase of 20–30% and 50% in the estimated intrinsic intestinal or hepatic clearance, respectively, and vice versa without profound changes in extraction ratio and bioavailability. Changes in intestinal length (which contributes to the flow term in the gut wall (Q_{gut}), that accounts for the permeability through the enterocyte (CL_{perm}) and the villous blood flow (Q_{vi})) did not result in different blood concentrations (change <1%), although the re-estimated intrinsic clearance in the gut wall changed +18 or −32% for an increase or decrease in intestinal length, respectively. The change in fraction unbound in blood for either midazolam or 1-OH-midazolam was inversely correlated with the same fractional change in estimated hepatic intrinsic clearance.

DISCUSSION

Using a physiological population PK model in which both physiological information and midazolam and metabolite concentrations after oral and intravenous administration were used, we were able to distinguish between intestinal and hepatic intrinsic clearance of midazolam in preterm neonates. The PK data used to estimate the CYP3A-mediated midazolam clearance came from a unique dataset with a crossover design in which preterm neonates received both an oral and an intravenous dose, allowing to study both the first-pass and systemic metabolism. Our physiological population PK modeling approach, which has already been applied in healthy adults,[22] was also able to describe the absorption and disposition of midazolam in preterm neonates. The results show that the CYP3A-mediated intrinsic gut clearance is much lower than the intrinsic hepatic clearance (**Table 2, Figure 2a**), whereas in healthy adult volunteers this difference is reported to be smaller (ratio of ~340 in preterm neonates vs. 60 in adults).[22] Although this indicates a difference in maturation of CYP3A activity in the gut wall and the liver in preterm neonates, both the intestinal and hepatic extraction ratio of midazolam in preterm neonates were very low (median of 0.04 each). This results in a very small first-pass effect leading to a high total bioavailability of 92.1% (**Figure 3**) and almost identical concentration-time profiles after intravenous and oral administration (**Figure 4a**) for the CYP3A-substrate midazolam in preterm neonates. For the metabolite, however, an increased plasma concentration can be observed in the first 4 hours after oral administration due to the presystemic formation of the metabolite in both the gut wall and liver (**Figure 4b**). In adults, much higher median extraction ratios of 0.59 and 0.34 have been reported for the gut wall and the liver, respectively,[22] resulting in a lower total bioavailability of around 30% in adults.

The intrinsic gut wall clearance values we obtained in preterm neonates were found to be lower than the values reported in adults. Additionally, in preterm neonates, the intrinsic gut wall clearance was much lower than the intrinsic hepatic clearance, and this difference was much larger in preterm neonates than in adults.[22] This could be due to

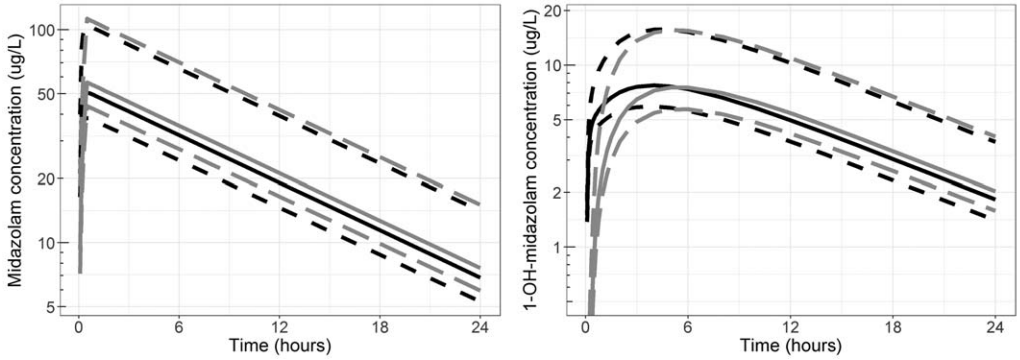

Figure 4 Model-based simulations of midazolam (**a**) and 1-OH-midazolam (**b**) pharmacokinetic profiles following a 0.1 mg/kg dose via an 30-minute infusion (gray lines) or orally (black lines). The solid lines represent the median plasma concentrations and the dashed lines show the minimal and maximal achieved concentrations of midazolam in the studied population.

the immaturity of enterocytic CYP3A enzyme activity in this population.[36,37] The activity in the gut wall has been reported to be lower with decreasing age,[37] but also conflicting activity values have been reported.[36] Besides the activity, the abundance of the CYP3A enzyme, reflected by a smaller number of milligrams of microsomal protein per gram of intestine,[37] as well as the smaller intestinal surface area led to a lower total intestinal CYP3A activity in preterm neonates compared with adults. The smaller surface area was calculated in our study based on intestinal length (70–157 cm for infants with a postconceptional age of 24–40 weeks without gastrointestinal malformations undergoing laparotomy,[27] which is in agreement with other literature[38,39] and on the mean intestinal radius of 1 cm.[26] A sensitivity analysis showed that with a decreased intestinal length, both the flow term that accounts for villous blood flow and permeability (Q_{gut}) and the gut wall clearance ($CL_{G,int}$) decreased, resulting in the same reported extraction ratio of 0.04. Furthermore, preterm infants have an underdeveloped intestinal barrier,[15] and neonates with a gestational age $<$34 weeks have a higher intestinal permeability,[16] which could be due to differences in the intracellular structures that regulate the intestinal permeability.[40] In our model, the permeability factor CL_{perm}[25] accounts for the intestinal surface area and the permeability of the intestinal barrier in preterm neonates. Food in the gastrointestinal tract may alter the gastrointestinal physiology, including the motility patterns, intestinal transit time, and the local blood flow,[41] but was not accounted for in our model because the exact times of parenteral and enteral feeding were not recorded during the study.

The intrinsic hepatic clearance obtained in our study in preterm neonates was very low compared with reported values in healthy adults (6.7 L/h and 1,620 L/h in preterm neonates and adults, respectively).[22] The neonatal liver is relatively immature shortly after birth, and its functional capacity in bile synthesis, detoxification, and metabolism increases during the early postnatal period.[42] Fetal and neonatal livers have different bile acid synthetic pathways than adult livers, and the bile acid pool is reduced,[42] limiting the probability of biliary excretion and enterohepatic recirculation of drugs in preterm neonates. The maturation of liver function is not a linear process, as the drug metabolizing enzyme expression changes nonlinearly during development.[3] In the fetal liver, 30–60% of adult values in cytochrome P450 content is found and the total hepatic CYP content increases after birth.[43] Of these CYP enzymes, the CYP3A family is the most abundant.[8,13,44] The CYP3A isoforms show a different ontogeny profile, with CYP3A4 activity increasing in preterm neonates with increasing age, CYP3A5 activity seems to be stable from neonatal life to adulthood, whereas simultaneously CYP3A7 activity declines in neonates.[44] Within the group of preterm neonates included in this study,[19,20] we could not identify a trend in hepatic intrinsic clearance with gestational age or postnatal age, which can be explained by the small age range of the studied population. Due to the lower intrinsic hepatic clearance, the hepatic extraction ratio is very low in preterm neonates compared with adults, resulting in a much higher hepatic bioavailability than expected based on adult values. This has been previously reported by Salem *et al*.[45] who found that the hepatic extraction ratio of midazolam increased with age. They found that the ontogeny of hepatic enzyme abundance and to a lesser extent the smaller number of microsomal protein per gram of liver contributed to the observed differences between preterm neonates and adults.[45] Based on the hepatic intrinsic clearance, the hepatic blood flow, the fraction unbound in blood, and the blood:plasma ratio, the total plasma clearance can be calculated (Eq. 8). The plasma clearance ranged from 0.03 to 0.79 L/h with a median value of 0.181 L/h (**Figure 2b**). This is in agreement with other reported values of 3.9 mL/min (0.23 L/h) for preterm neonates with a mean gestational age of 32.1 ± 2.8 weeks[12] and higher than the reported values of 0.783 mL/min (0.05 L/h) and 0.104 L/h in very premature neonates with a mean gestational age of 27 (24–31) and 27.9 (25–30) weeks, respectively.[46,47]

The RSE percentage for the estimated intrinsic gut wall clearance value and high range of the 90% bootstrap confidence interval of this parameter together with a high number of unsuccessful runs in the bootstrap and a high condition number suggest overparameterization of the model. In a population modeling approach, this could warrant a re-evaluation of the structural model, however, our structural model and a subset of parameter values are based on physiological knowledge and physiologically based pharmacokinetic principles, and only the values of the remaining subset of parameters were estimated from concentration-time data using population modeling principles. The high RSE% and 90% bootstrap confidence interval can, therefore, be interpreted to mean that the data do not support a very precise estimate of intrinsic gut wall clearance.

For the structural model a few assumptions were included, which were evaluated in a sensitivity analysis. Plasma albumin concentrations were calculated based on a reported age-based formula by Johnson *et al*.[5] in term neonates, assuming the preterm neonates to have the same concentrations as a 1-day-old term neonate. In addition, only plasma albumin concentrations were taken into account. Free fatty acid (FFA) concentrations are known to reduce protein binding of diazepam in neonates,[48] and could result in a higher fraction unbound in blood for midazolam as well, but this was not taken into account, nor were other factors that could impact protein binding of midazolam. Our findings about the low gut wall and hepatic extraction leading to a small first-pass effect and high bioavailability in preterm neonates are, however, not influenced by these assumptions. Even though the fraction unbound and the intrinsic hepatic clearances are related, a different fraction unbound would increase the intrinsic clearance proportionally, yielding no net changes in extraction ratio or bioavailability. Furthermore, tissue volumes and organ blood flows are not directly measurable in preterm neonates. Therefore, allometric scaling was applied to scale the organ blood flows from data in term neonates[7] to preterm neonates. The sensitivity analysis showed that changes in assumed organ blood flow are correlated with the estimated organ clearances: with an increased intestinal blood flow, the intrinsic intestinal clearance was estimated higher and

the assumptions of the hepatic blood flow were found to correlate with the estimated intrinsic hepatic clearance. However, in this study, also the extraction ratios and bioavailability derived from the estimated parameter values remained unaffected by changes in organ blood flows and would, therefore, not have an impact on our finding that the first-pass midazolam in preterm neonates is much smaller than in adults.

To conclude, the developed physiological population PK model was able to distinguish between CYP3A-mediated intestinal and hepatic metabolism of midazolam in preterm neonates. Intrinsic clearance in the gut wall was much lower than in the liver, but the median intestinal and hepatic bioavailability were both very high. This indicates a very low first-pass effect by intestinal and hepatic CYP3A-mediated metabolism in preterm neonates compared with adults. Furthermore, the variability in bioavailability was very high, indicating that oral dosing may yield large differences in drug exposure within this population. Overall, the PK of midazolam and its primary metabolite 1-OH-midazolam were well-described by the model, and this physiological model may, therefore, be used to predict the first-pass effect and systemic metabolism of midazolam and other orally administered CYP3A substrates in preterm neonates based on the physiological and drug properties.

Source of Funding. C.A.J. Knibbe was supported by an NWO Vidi grant (Knibbe 2013).

Conflict of Interest. The authors declared no competing interests for this work.

Author Contributions. J.M.B., H.Y., E.H.J.K., B.d.R., M.J.E.B., J.N.v.d.A., A.R.-H., S.N.d.W., and C.A.J.K. wrote the manuscript. J.M.B., E.H.J.K., S.N.d.W., and C.A.J.K. designed the research. J.M.B., H.Y., E.H.J.K., B.d.R., M.J.E.B., J.N.v.d.A., S.N.d.W., and C.A.J.K. performed the research. J.M.B., H.Y., and B.d.R. analyzed the data.

1. Kearns, G.L. Impact of developmental pharmacology on pediatric study design: overcoming the challenges. *J. Allergy Clin. Immunol.* **106**(3 suppl), S128–S138 (2000).
2. O'Hara, K., Wright, I.M., Schneider, J.J., Jones, A.L. & Martin, J.H. Pharmacokinetics in neonatal prescribing: evidence base, paradigms and the future. *Br. J. Clin. Pharmacol.* **80**, 1281–1288 (2015).
3. Allegaert, K., van den Anker, J.N., Naulaers, G. & de Hoon, J. Determinants of drug metabolism in early neonatal life. *Curr. Clin. Pharmacol.* **2**, 23–29 (2007).
4. Johnson, P.J. Neonatal pharmacology—pharmacokinetics. Neonatal Netw. **30**, 54–61 (2011).
5. Johnson, T.N., Rostami-Hodjegan, A. & Tucker, G.T. Prediction of the clearance of eleven drugs and associated variability in neonates, infants and children. *Clin. Pharmacokinet.* **45**, 931–956 (2006).
6. McNamara, P.J. & Alcorn, J. Protein binding predictions in infants. *AAPS PharmSci.* **4**, E4 (2002).
7. Björkman, S. Prediction of drug disposition in infants and children by means of physiologically based pharmacokinetic (PBPK) modelling: theophylline and midazolam as model drugs. *Br. J. Clin. Pharmacol.* **59**, 691–704 (2005).
8. de Wildt, S.N., Kearns, G.L., Leeder, J.S. & van den Anker, J.N. Cytochrome P450 3A: ontogeny and drug disposition. *Clin. Pharmacokinet.* **37**, 485–505 (1999).
9. Thummel, K.E. *et al.* Use of midazolam as a human cytochrome P450 3A probe: I. In vitro-in vivo correlations in liver transplant patients. *J. Pharmacol. Exp. Ther.* **271**, 549–556 (1994).
10. Gorski, J.C., Hall, S.D., Jones, D.R., VandenBranden, M. & Wrighton, S.A. Regioselective biotransformation of midazolam by members of the human cytochrome P450 3A (CYP3A) subfamily. *Biochem. Pharmacol.* **47**, 1643–1653 (1994).
11. Hall, R.W. & Shbarou, R.M. Drugs of choice for sedation and analgesia in the neonatal ICU. *Clin. Perinatol.* **36**, 15–26 (2009).
12. Jacqz-Aigrain, E., Daoud, P., Burtin, P., Maherzi, S. & Beaufils, F. Pharmacokinetics of midazolam during continuous infusion in critically ill neonates. *Eur. J. Clin. Pharmacol.* **42**, 329–332 (1992).
13. Ince, I., Knibbe, C.A., Danhof, M. & de Wildt, S.N. Developmental changes in the expression and function of cytochrome P450 3A isoforms: evidence from in vitro and in vivo investigations. *Clin. Pharmacokinet.* **52**, 333–345 (2013).
14. Debotton, N. & Dahan, A. A mechanistic approach to understanding oral drug absorption in pediatrics: an overview of fundamentals. *Drug Discov. Today* **19**, 1322–1336 (2014).
15. Anderson, R.C., Dalziel, J.E., Gopal, P.K., Bassett, S., Ellis, A. & Roy, N.C. The role of intestinal barrier function in early life in the development of colitis. *Colitis* (ed. Fukata, M.) (InTech, London, UK, 2012).
16. Weaver, L.T., Laker, M.F. & Nelson, R. Intestinal permeability in the newborn. *Arch. Dis. Child.* **59**, 236–241 (1984).
17. Tsamandouras, N., Rostami-Hodjegan, A. & Aarons, L. Combining the 'bottom up' and 'top down' approaches in pharmacokinetic modelling: fitting PBPK models to observed clinical data. *Br. J. Clin. Pharmacol.* **79**, 48–55 (2015).
18. Rostami-Hodjegan, A. Reverse translation in PBPK and QSP: going backwards in order to go forward with confidence. *Clin. Pharmacol. Ther.* **103**, 224–232 (2018).
19. de Wildt, S.N., Kearns, G.L., Hop, W.C., Murry, D.J., Abdel-Rahman, S.M. & van den Anker, J.N. Pharmacokinetics and metabolism of intravenous midazolam in preterm infants. *Clin. Pharmacol. Ther.* **70**, 525–531 (2001).
20. de Wildt, S.N., Kearns, G.L., Hop, W.C., Murry, D.J., Abdel-Rahman, S.M. & van den Anker, J.N. Pharmacokinetics and metabolism of oral midazolam in preterm infants. *Br. J. Clin. Pharmacol.* **53**, 390–392 (2002).
21. Yang, J., Kjellsson, M., Rostami-Hodjegan, A. & Tucker, G.T. The effects of dose staggering on metabolic drug-drug interactions. *Eur. J. Pharm. Sci.* **20**, 223–232 (2003).
22. Frechen, S. *et al.* A semiphysiological population pharmacokinetic model for dynamic inhibition of liver and gut wall cytochrome P450 3A by voriconazole. *Clin. Pharmacokinet.* **52**, 763–781 (2013).
23. Brill, M.J. *et al.* Semiphysiologically based pharmacokinetic model for midazolam and CYP3A mediated metabolite 1-OH-midazolam in morbidly obese and weight loss surgery patients. *CPT Pharmacometrics Syst. Pharmacol.* **5**, 20–30 (2016).
24. Aguirre-Reyes, D.F. *et al.* Intrahepatic portal vein blood volume estimated by non-contrast magnetic resonance imaging for the assessment of portal hypertension. *Magn. Reson. Imaging* **33**, 970–977 (2015).
25. Yang, J., Jamei, M., Yeo, K.R., Tucker, G.T. & Rostami-Hodjegan, A. Prediction of intestinal first-pass drug metabolism. *Curr. Drug Metab.* **8**, 676–684 (2007).
26. Ives, G.C., Demehri, F.R., Sanchez, R., Barrett, M., Gadepalli, S. & Teitelbaum, D.H. Small bowel diameter in short bowel syndrome as a predictive factor for achieving enteral autonomy. *J. Pediatr.* **178**, 275–277 (2016).
27. Struijs, M.C., Diamond, I.R., de Silva, N. & Wales, P.W. Establishing norms for intestinal length in children. *J. Pediatr. Surg.* **44**, 933–938 (2009).
28. Ito, K., Ogihara, K., Kanamitsu, S. & Itoh, T. Prediction of the in vivo interaction between midazolam and macrolides based on in vitro studies using human liver microsomes. *Drug Metab. Dispos.* **31**, 945–954 (2003).
29. Mandema, J.W., Tuk, B., van Steveninck, A.L., Breimer, D.D., Cohen, A.F. & Danhof, M. Pharmacokinetic-pharmacodynamic modeling of the central nervous system effects of midazolam and its main metabolite alpha-hydroxymidazolam in healthy volunteers. *Clin. Pharmacol. Ther.* **51**, 715–728 (1992).
30. Maharaj, A.R., Barrett, J.S. & Edginton, A.N. A workflow example of PBPK modeling to support pediatric research and development: case study with lorazepam. *AAPS J.* **15**, 455–464 (2013).
31. Irwin, J.J. & Kirchner, J.T. Anemia in children. *Am. Fam. Physician* **64**, 1379–1386 (2001).
32. Basic anatomical and physiological data for use in radiological protection reference values. A report of age- and gender-related differences in the anatomical and physiological characteristics of reference individuals. ICRP Publication 89. *Ann. ICRP.* **32**, 5–265 (2002).
33. Yang, J., Jamei, M., Yeo, K.R., Rostami-Hodjegan, A. & Tucker, G.T. Misuse of the well-stirred model of hepatic drug clearance. *Drug Metab. Dispos.* **35**, 501–502 (2007).
34. Bellu, G., Saccomani, M.P., Audoly, S. & D'Angiò, L. DAISY: a new software tool to test global identifiability of biological and physiological systems. *Comput. Methods Programs Biomed.* **88**, 52–61 (2007).
35. Krause, A. & Lowe, P.J. Visualization and communication of pharmacometric models with Berkeley Madonna. *CPT Pharmacometrics Syst. Pharmacol.* **3**, e116 (2014).
36. Fakhoury, M. *et al.* Localization and mRNA expression of CYP3A and P-glycoprotein in human duodenum as a function of age. *Drug Metab. Dispos.* **33**, 1603–1607 (2005).
37. Johnson, T.N., Tanner, M.S., Taylor, C.J. & Tucker, G.T. Enterocytic CYP3A4 in a paediatric population: developmental changes and the effect of coeliac disease and cystic fibrosis. *Br. J. Clin. Pharmacol.* **51**, 451–460 (2001).
38. Archie, J.G., Collins, J.S. & Lebel, R.R. Quantitative standards for fetal and neonatal autopsy. *Am. J. Clin. Pathol.* **126**, 256–265 (2006).

39. Touloukian, R.J. & Smith, G.J. Normal intestinal length in preterm infants. *J. Pediatr. Surg.* **18**, 720–723 (1983).
40. Halpern, M.D. & Denning, P.W. The role of intestinal epithelial barrier function in the development of NEC. *Tissue Barriers* **3**, e1000707 (2015).
41. Abuhelwa, A.Y., Williams, D.B., Upton, R.N. & Foster, D.J. Food, gastrointestinal pH, and models of oral drug absorption. *Eur. J. Pharm. Biopharm.* **112**, 234–248 (2017).
42. Grijalva, J. & Vakili, K. Neonatal liver physiology. *Semin. Pediatr. Surg.* **22**, 185–189 (2013).
43. Hines, R.N. & McCarver, D.G. The ontogeny of human drug-metabolizing enzymes: phase I oxidative enzymes. *J. Pharmacol. Exp. Ther.* **300**, 355–360 (2002).
44. de Wildt, S.N. Profound changes in drug metabolism enzymes and possible effects on drug therapy in neonates and children. *Expert Opin. Drug Metab. Toxicol.* **7**, 935–948 (2011).
45. Salem, F., Abduljalil, K., Kamiyama, Y. & Rostami-Hodjegan, A. Considering age variation when coining drugs as high versus low hepatic extraction ratio. *Drug Metab. Dispos.* **44**, 1099–1102 (2016).
46. Lee, T.C., Charles, B.G., Harte, G.J., Gray, P.H., Steer, P.A. & Flenady, V.J. Population pharmacokinetic modeling in very premature infants receiving midazolam during mechanical ventilation: midazolam neonatal pharmacokinetics. *Anesthesiology* **90**, 451–457 (1999).
47. Harte, G.J., Gray, P.H., Lee, T.C., Steer, P.A. & Charles, B.G. Haemodynamic responses and population pharmacokinetics of midazolam following administration to ventilated, preterm neonates. *J. Paediatr. Child Health* **33**, 335–338 (1997).
48. Nau, H., Luck, W. & Kuhnz, W. Decreased serum protein binding of diazepam and its major metabolite in the neonate during the first postnatal week relate to increased free fatty acid levels. *Br. J. Clin. Pharmacol.* **17**, 92–98 (1984).

Supplementary information accompanies this paper on the *CPT: Pharmacometrics & Systems Pharmacology* website (http://psp-journal.com)